

Telling twins apart: exo-Earths and Venuses with transit spectroscopy

J. K. Barstow,^{1,2★} S. Aigrain,¹ P. G. J. Irwin,² S. Kendrew¹ and L. N. Fletcher³

¹*Department of Physics, Astrophysics, Denys Wilkinson Building, University of Oxford, Keble Road, Oxford OX1 3RH, UK*

²*Department of Physics, Atmospheric, Oceanic and Planetary Physics, Clarendon Laboratory, University of Oxford, Parks Road, Oxford OX1 3PU, UK*

³*Department of Physics and Astronomy, University of Leicester, University Road, Leicester LE1 7RH, UK*

Accepted 2016 February 26. Received 2016 February 26; in original form 2015 December 2

ABSTRACT

The planned launch of the *James Webb Space Telescope (JWST)* in 2018 will herald a new era of exoplanet spectroscopy. *JWST* will be the first telescope sensitive enough to potentially characterize terrestrial planets from their transmission spectra. In this work, we explore the possibility that terrestrial planets with Venus-type and Earth-type atmospheres could be distinguished from each other using spectra obtained by *JWST*. If we find a terrestrial planet close to the liquid water habitable zone of an M5 star within a distance of 10 parsec, it would be possible to detect atmospheric ozone if present in large enough quantities, which would enable an oxygen-rich atmosphere to be identified. However, the cloudiness of a Venus-type atmosphere would inhibit our ability to draw firm conclusions about the atmospheric composition, making any result ambiguous. Observing small, temperate planets with *JWST* requires significant investment of resources, with single targets requiring of the order of 100 transits to achieve sufficient signal to noise. The possibility of detecting a crucial feature such as the ozone signature would need to be carefully weighed against the likelihood of clouds obscuring gas absorption in the spectrum.

Key words: radiative transfer – methods: data analysis – planets and satellites: atmospheres.

1 INTRODUCTION

The field of exoplanet science has been transformed over the last few years, with discoveries of water vapour (e.g. Wakeford et al. 2013; Madhusudhan et al. 2014), alkali metals (e.g. Redfield et al. 2008) and even clouds (e.g. Pont et al. 2013; Kreidberg et al. 2014) in the atmospheres of exotic worlds. The majority of these discoveries were made using the transit spectroscopy technique. When a planet transits in front of its parent star, it blocks a small fraction of the starlight; gases or particulates in planet’s atmosphere absorb or scatter starlight at particular wavelengths, meaning that the fraction of light blocked varies as a function of wavelength.

Currently, the majority of transiting exoplanets for which we have atmospheric information are hot Jupiters, because their size and extended atmospheres produce a large transit spectroscopy signal. Reported discoveries of ‘Earth-like planets’ from the *Kepler* mission rest on assumptions based on their measured sizes, and estimates of the planets’ temperatures from their orbital periods. However, the conditions on a planet’s surface are dependent on the atmospheric properties as well as the distance from the star, and in particular calculations of the extent of the Solar system liquid water habitable zone (HZ) are model-dependent and show some disagreement. Recent calculations by Kopparapu et al. (2013) using a 1D, cloud-free climate model indicate that the Earth is very close to

the inner edge of the HZ, which in this model is located 0.99 AU from the Sun, and Venus is well outside it; however, modelling by Zsom et al. (2013) indicates that for certain conditions of humidity, surface pressure and surface albedo the HZ could extend as far in as 0.38 AU. In addition, 3D models presented by Leconte et al. (2013) indicate that tidally locked planets that might otherwise experience a runaway greenhouse may actually have stable liquid water in cold traps on the nightside.

Estimating habitability based on orbital period and planet size might work in our own Solar system today, but Venus is approximately Earth-sized and may have been in the HZ as recently as 1 billion years ago (Abe et al. 2011). Therefore, it involves risky assumptions for exoplanetary systems. However, the development of larger and more sensitive telescopes over the next few years should make it easier to target smaller, denser planets for spectroscopic follow-up observations. Whilst the spectral signals of interest for Earth-size planets transiting sun-like stars are too small relative to the star’s brightness, of the order of 1:1000000, Earth-sized planets around smaller M dwarf stars may have large enough signals. In addition, the much smaller orbital radius of the HZ around these cool stars means temperate planets have short periods, making it easier to combine multiple observations to boost the signal.

The *James Webb Space Telescope (JWST)*, due to launch in 2018 with a 25 m² primary mirror, may be capable of characterizing the atmosphere of an Earth-sized planet orbiting an M dwarf, should such a system be found in our near neighbourhood (within 10 pc). Surveys such as Transiting Exoplanet Survey Satellite (TESS) (Ricker

* E-mail: joannakarstow@cantab.net

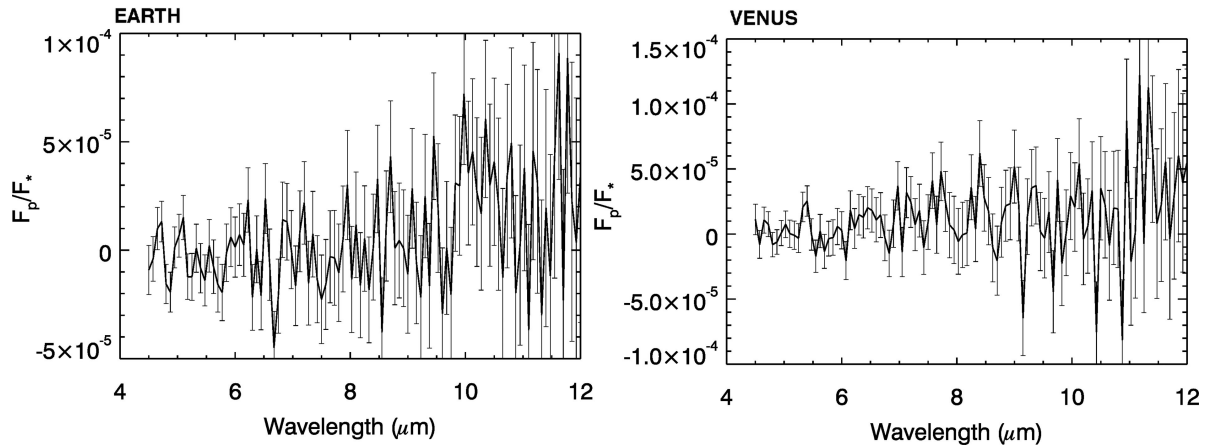


Figure 1. Secondary eclipse spectra with *JWST*/MIRI for Earth and Venus around an M5 star at 10 pc. Spectra are averaged over 30 (50) eclipses for Earth (Venus). The low signal to noise means that very little information is obtainable from these spectra.

2015) and the Next Generation Transit Survey (Wheatley 2013), which are optimised for detecting transits around red stars, may discover such planets. Deming et al. (2009), Kaltenegger & Traub (2009) and Barstow et al. (2015) showed that it might be possible to detect ozone in the atmosphere of an Earth analogue planet in orbit around an M dwarf, but full characterization of the atmosphere’s composition and structure is likely to be difficult even for a favourable case. However, detection of ozone is in itself of interest, especially for a planet in the HZ of its parent star, as it might indicate that the planet has an Earth-like atmosphere. Simulating Venus in transit (as e.g. Ehrenreich et al. 2012) indicates which features might be observable for this more inhospitable world.

In this paper, we investigate whether it would be possible to distinguish between an Earth-analogue planet and a Venus-analogue planet orbiting an M dwarf, using transmission spectra obtained by *JWST*. At first glance, the atmospheres of Earth and Venus are very different, but in transmission geometry, light penetrates to a limited depth in the atmosphere, especially if clouds are present (e.g. the case of super-Earth GJ 1214b; Kreidberg et al. 2014). Both planets are cloudy, so this may mask their atmospheric composition differences in transmission spectra. Secondary transit spectra for these planets have low signal to noise, even when averaged over several tens of eclipses (Fig. 1).

2 EARTH AND VENUS

Earth and Venus are the fraternal twins of the Solar system. They are similarly sized rocky bodies (Venus has a radius of $0.95 R_{\oplus}$), and both exist either within or close to the liquid water HZ. Even though Venus is closer to the Sun, because it is highly reflective it has a slightly lower equilibrium temperature of ~ 250 K compared with Earth’s 260 K.

However, the similarities end here. Venus has a much higher surface temperature and pressure than Earth, 735 K and 92 bars, respectively, compared with around 287 K and 1 bar for Earth. At some point in its past, Venus’s atmosphere entered a runaway greenhouse phase, during which the majority of its water was lost (Rasool & de Bergh 1970; Donahue et al. 1982). Without any surface water to facilitate carbonate rock formation, almost all of Venus’s carbon budget is in the atmosphere in the form of CO_2 , making up 96 per cent of the total atmospheric volume. This accounts for the extreme surface conditions. Due to the loss of water, Venus’s atmosphere is very dry compared with Earth’s, but it does have cloud

and haze made of sulphuric acid (H_2SO_4 ; Hansen & Hovenier 1974; Pollack et al. 1974). The sulphuric acid aerosols are formed as a photochemical product of SO_2 gas and the little water vapour that is present. Venus’s atmosphere has high concentrations of sulphur gases such as SO_2 and OCS, probably as a result of significant past or current volcanic activity. It is however lacking in bio-activity-related gases O_2 and ozone, which are present in significant quantities on Earth (see Taylor & Grinspoon 2009, for a summary of Venusian climate).

A detailed understanding of their atmospheres is needed to reveal the very different surface conditions on Venus and Earth. Identifying an Earth analogue planet using transit spectroscopy will therefore require Venus-like scenarios to be ruled out. It may be possible, using the soon-to-be-launched *JWST*, to identify absorption features due to key gases and distinguish between Venus-like and Earth-like atmospheres.

3 SYNTHETIC SPECTRA

Synthetic spectra for Earth and Venus were produced using the *NEMESIS* radiative transfer and retrieval code (Irwin et al. 2008). *NEMESIS* contains a 1D radiative transfer model that incorporates a rapid correlated-k (Lacis & Oinas 1991, after Goody & Yung 1989) radiative transfer scheme, and an optimal estimation retrieval algorithm (Rodgers 2000). Properties specified in the forward models include temperature and atmospheric gas abundances as a function of pressure, cloud specific density and wavelength-dependent extinction cross-section, and planet mass and radius. The stellar radius is also specified and becomes important in the calculation of transit depth.

The analogue planets are based on the current atmospheric compositions of Earth and Venus; we assume that they evolved in exactly the same way as Earth and Venus did in the Solar system, so they have identical atmospheric characteristics. The validity of this assumption, and possible alternatives, are explored in Section 7. The Earth model used is as presented in Irwin et al. (2014), and the Venus model is based on that used in Barstow et al. (2012), after Seiff et al. (1985). Line data for both planets are taken from the HITRAN08 data base (Rothman 2009). Sulphuric acid refractive indices for the Venus cloud model are taken from Palmer & Williams (1975) ($\lambda < 5 \mu\text{m}$) and Myhre et al. (2003) ($\lambda > 5 \mu\text{m}$). Whilst it is usually necessary to use high-temperature line data bases for Venus, due to the long path length in transmission geometry transit spectra

are insensitive to the atmosphere below the 1 bar level, which on Venus corresponds to around 50 km. The high-temperature portion of the Venusian atmosphere is effectively inaccessible and therefore high-temperature line data are not required in this case.

Both models are based on the best-fitting atmospheric composition, structure and cloud properties for each planet. The only exception is the introduction of a reduced cloud opacity model for Venus, to test the sensitivity to the presence of cloud. Whereas clouds on Earth are patchy and the cloud top pressure is rarely lower than 100 mbar (e.g. measurements from the Spinning-Enhanced Visible InfraRed Imager satellite analysed by Hamann et al. 2014), the cloud layer on Venus is permanently present and extends up to the 1 mbar level (see Esposito et al. 1983 for a summary of the major features). This means that the higher, thicker Venusian cloud will have a much larger impact on transmission spectra than the Earth cloud. An example of the effect of increasing cloud top altitude on transmission spectra is shown by B  tr  mieux & Kaltene  ger (2014), with increasingly higher cloud top altitudes for an Earth-like planet resulting in smaller and smaller molecular absorption features; Barstow et al. (2013b) shows the same effect for the super-Earth exoplanet GJ 1214b.

The planets are assumed to be in orbit around a 3000 K M5 red dwarf with a radius of $0.14 R_{\odot}$ and a mass of $0.122 M_{\odot}$. We calculate that, for the planets to have the same equilibrium temperature as they do in the Solar system, Venus and Earth would be in orbits of ~ 5 and 8 d, respectively. This would make it possible to observe the planets in transit many times during the lifetime of *JWST*.

4 NOISE MODEL

Noise is added to the spectra using the same methods and instrument characteristics as those presented in Barstow et al. (2015). As in the previous work, the simulated spectra are based on a prism mode observation with the NIRSpec instrument, covering 0.6 to $5 \mu\text{m}$, and a Mid-InfraRed Instrument (MIRI) low-resolution spectrograph observation covering 4.5–12 μm . In this paper, we do not consider the effect of systematic errors and starspots; we refer the reader to Barstow et al. (2015) for a detailed discussion of these issues for *JWST*, and discuss the possible impacts on this case in Section 7.

The noise for both instruments is calculated assuming the photon noise limit is reached, using the equation

$$n_{\lambda} = I_{\lambda} \times \pi \times (r_{*}/D_{*})^2 \times (\lambda/hc) \times (\lambda/R) \times A_{\text{eff}} \times QE \times \eta \times t, \quad (1)$$

where n_{λ} is the number of photons received for a given wavelength λ , I_{λ} is the spectral radiance of the stellar signal, r_{*} is the stellar radius, D_{*} is the distance to the star, h and c are the Planck constant and speed of light, R is the spectral resolving power, A_{eff} is the telescope effective area, QE is the detector quantum efficiency, η is the throughput and t is the exposure time. For NIRSpec, we adopt the average transmission and quantum efficiency properties used by Deming et al. (2009), assuming a detector QE of 0.8, a telescope optics efficiency of 0.88 and a total NIRSpec optics transmission of 0.4. For MIRI-LRS, we use the photon conversion efficiency presented in Kendrew et al. (2015). This is the fraction of photons from the source that are eventually received and recorded by the detector, combining the QE and throughput. The total area of the primary mirror is 25 m^2 . Exposure time is equal to the transit duration across the stellar equator for the assumed orbits, with an assumption of an 80 per cent duty cycle as used in previous work (Barstow et al. 2013a, 2015).

Although the planet:star size ratio is favourable for these cases, M5 stars are cool and therefore relatively faint. Even for a nearby star, multiple observations would be required with *JWST*. The models presented assume 30 observations (50 for Venus) each with MIRI and NIRSpec, for planets orbiting an M5 star at 10 pc distance. MIRI and NIRSpec cannot be used to observe simultaneously, so this translates to 60 (100) observations per planet in total, of around 3 h each including the out-of-transit baseline. This would be easily feasible in the lifetime of *JWST* due to the short orbital periods of both planets, but it would clearly be a major investment of valuable observational time.

These values can be compared with the condition adopted by Deming et al. (2009) that 60 transits would be reasonable to characterize a habitable $10 M_{\oplus}$ super-Earth. The size of observable atmospheric signals remains relatively constant from Earth through to super-Earth-sized objects, since the effects of increased gravity/smaller atmospheric scaleheight offset the increased area of the transiting planet. Deming et al. (2009) estimate that TESS would discover between 1 and 5 habitable super-Earths for which H_2O and CO_2 absorption could be characterized using *JWST*. Kaltene  ger & Traub (2009) found that multiple transits would be required to detect O_3 in the atmosphere of an Earth-analogue planet around an M dwarf, finding a signal-to-noise ratio of 20 could be achieved for the infrared O_3 feature with 200 h of in-transit observation.

5 RETRIEVAL TESTS

The aim of this study is to test whether it is possible to distinguish between Earth-like and Venus-like atmospheres of terrestrial exoplanets. In the majority of cases, where the planet is at least partially cloudy, it is virtually impossible to recover the full atmospheric state from a transit spectrum due to degeneracies between bulk composition, cloud and temperature (see e.g. Benneke & Seager 2012; Barstow et al. 2013a,b, and Griffith 2014 for a useful summary). Therefore, what we are interested in is not an accurate recovery of the atmospheric state vector, rather it is whether or not the synthetic observation can best be matched with a Venus- or Earth-like model atmosphere. It is of course also possible that an Earth-sized object in another Solar system may have evolved an atmosphere different from either of these; however, for purposes of comparative planetology, a key goal following the discovery of another terrestrial HZ planet would be to see whether it most closely resembles the temperate, habitable scenario found on Earth, or the Venus runaway greenhouse.

To this end, we perform retrieval tests for each planet with a range of nine model atmospheres, ranging from Venus-like to Earth-like with intermediate cases in between. Since there is little sensitivity to temperature in primary transit spectra, we use the same temperature profile (Fig. 2) in the retrieval model for both cases. The temperature mainly affects the scaleheight, which impacts the size but not the presence of gas absorption features, and Venus and Earth actually have broadly similar temperature–pressure profiles where they overlap in pressure, although the structure differs. This makes the test somewhat more realistic, as information about the temperature structure can only be obtained from secondary transit observations. Otherwise, it must be estimated *ab initio* from the equilibrium temperature, which would result in a similar profile to the one used. As shown in Fig. 1, secondary transit signal-to-noise for these objects is too small to obtain any useful information about temperature structure.

We include a combination of the gases expected to be found in Earth and Venus atmospheres in the retrieval models; H_2O , CO_2 ,

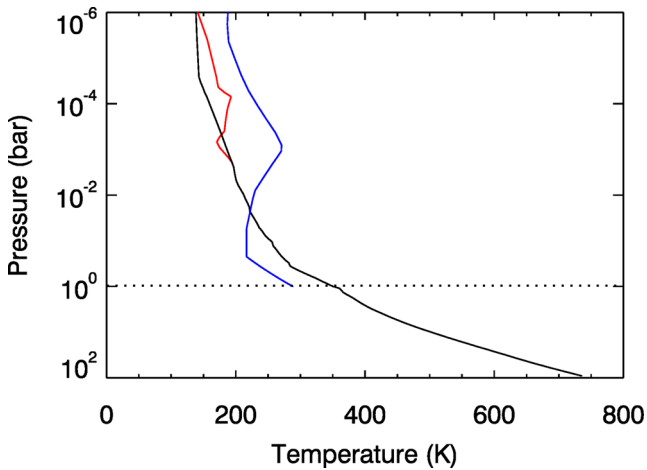


Figure 2. The temperature–pressure profile used in the retrievals (black) compared with the input profiles for Earth (blue) and Venus (red). The surface for the Earth profile is indicated by the dashed line. The profile used for the retrievals is a smoothed version of the Venus profile.

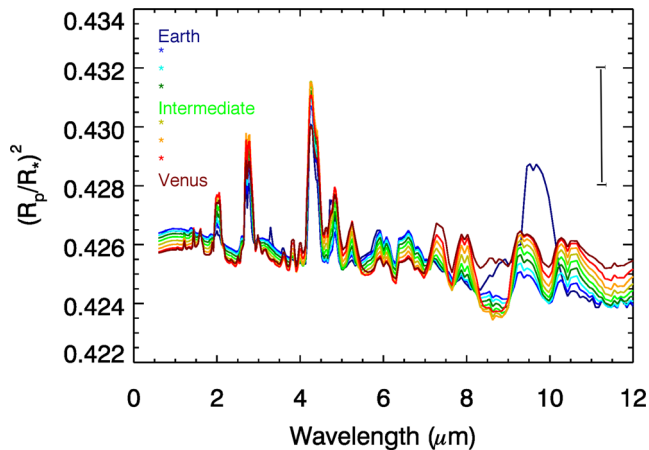


Figure 3. Synthetic spectra (for Earth bulk properties) for each of the nine atmospheric composition models. Note that the ozone feature at $9 \mu\text{m}$ is only large enough to be seen in the most Earth-like case (navy blue line), and an SO_2 can be seen in the dark red Venus-like spectrum at $8.5 \mu\text{m}$; however, this second feature is on the order of the noise, so in practice is unlikely to be observable. Noise is indicated by the bar on the right of the plot.

O_3 , CO , CH_4 , O_2 , SO_2 , OCS , and N_2 . We test a set of nine retrieval model atmospheres, ranging from the Earth case (78 per cent N_2 , 21 per cent O_2 , negligible SO_2 and OCS , significant O_3) to the Venus case (96 per cent CO_2 , 3.5 per cent N_2 , negligible O_2 and O_3 , including SO_2 and OCS). Seven intermediate models have intermediate abundance of each gas with even steps in log-space, except for N_2 which has no absorption lines and is used to bring the abundance total up to 100 per cent. The synthetic spectra corresponding to each of the nine models are shown in Fig. 3. The abundance priors for all gases except N_2 , for each of the nine models, are shown in Fig. 4. Because several gases are not included at all in the input model for either Earth or Venus, the a priori abundances for the retrieval can be as low as 10^{-36} . For these cases, where a gas is only considered to be present in either the Earth or Venus like atmosphere, the gas only has an observable effect on the spectrum close to either the Earth or Venus model end members.

For each planet, we run a separate retrieval with each of the nine atmospheric priors. We allow cloud optical depth and abundances of H_2O , CO_2 , O_3 , CO , CH_4 and O_2 to vary in the retrieval, and we retrieve scaling factors for all these quantities. The cloud prior for Venus is discussed later in Section 6. Precise abundances of SO_2 and OCS did not have a significant effect on the spectra, and in fact none of the retrieved gas abundances deviated very far from the a priori case during the retrieval, suggesting that there is little sensitivity to the precise abundance of each gas; however, as discussed in Section 6, we find that there is sensitivity to the presence or absence of certain gases.

We also retrieved the radius at the base of the atmosphere, in these cases at the planet’s surface. The reason for this is that the radius at a given pressure is not known for an exoplanet until the atmospheric state is also known; the pressure being probed at the white light transit radius depends on the gas absorbers present in the atmosphere and also the cloud top pressure. The molecular weight of the atmosphere depends on the model atmosphere composition and is calculated within *NEMESIS*.

For the Earth retrievals, we use an Earth-like water cloud model as included by Irwin et al. (2014), which has relatively little effect on the retrieval due to the low optical depth and deep cloud top. We test two different cloud models for the Venus retrieval – a Venus-like model based on Barstow et al. (2012) with optically thick cloud up to $\sim 80 \text{ km}$ altitude, and a reduced optical depth version of the same model which would have a much smaller effect on the spectrum. The reduced-OD model has the upper cloud optical depth reduced by a factor of 10 000 from cloudy Venus model, representing a significant clearing of the cloud.

6 RESULTS

We present results from the Earth test and from three Venus tests with different cloud properties and priors. χ^2 values, the synthetic observation and fitted spectra for Earth are shown in Fig. 5, and for Venus in Fig. 6. The number of degrees of freedom (measurements – number of variables) is 251.

In the Earth case, the Earth-like, ozone-containing model provides a much better fit than any other, with the lowest χ^2 (Fig. 5). This is because the ozone feature at $9 \mu\text{m}$ is clearly seen in the synthetic observation, and cannot be reproduced by combinations of other gases. This supports the findings briefly presented in Barstow et al. (2015), that the ozone feature could be detected in the atmosphere of an Earth twin around a small, cool star.

However, the case is less clear-cut for Venus. For the cloudy Venus-twin case with the cloudy model prior, the Venus model does produce the best fit, but the range of χ^2 values is far narrower than for the Earth case. This is because the thick cloud, extending up to the low-pressure region of the atmosphere, cuts off the majority of the gas absorption features; only the centre of the $4.3 \mu\text{m}$ CO_2 band is visible above the noise. This means the information available from the spectrum is very limited, so little constraint is provided on the properties of the atmosphere.

Due to the extreme flatness of the spectrum, if a reduced-cloud a priori model is used to fit the cloudy Venus spectrum, something quite strange happens (middle row, Fig. 6). The model with the lowest χ^2 is actually the Earth atmosphere model. Despite the fact that this model contains an ozone feature where none is seen in the spectrum, it fits well because the size of the $4.3 \mu\text{m}$ CO_2 absorption feature matches most closely. The CO_2 feature in the synthetic observation is small because the cloud prevents the deep wings of the feature from being seen. However, in the Earth model, the CO_2

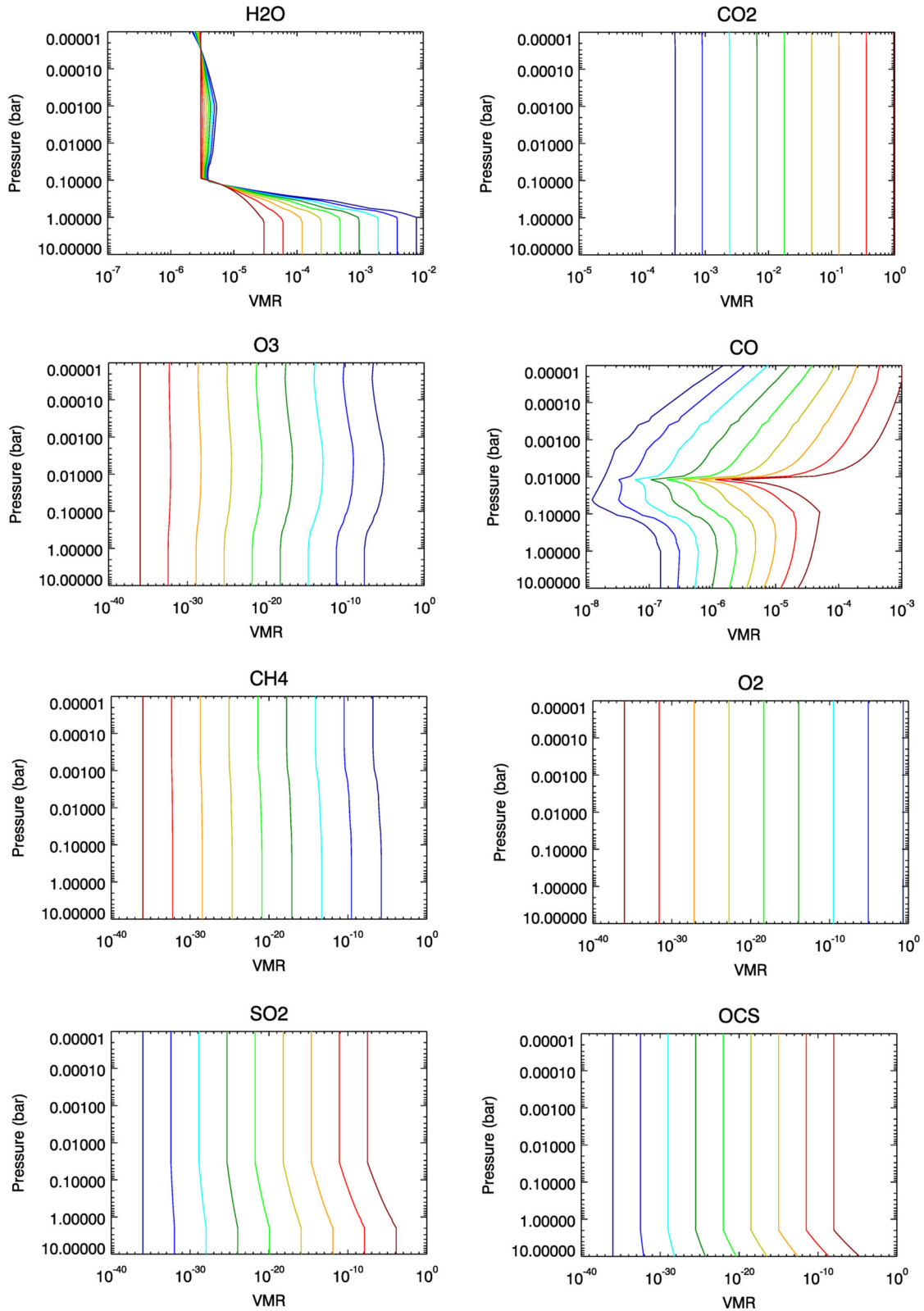


Figure 4. Gas abundance profiles for the Earth/Venus model atmospheres. The abundance of each gas is expressed as a volume mixing ratio (VMR), defined as the molecular number density of each gas over the total number density of atmospheric molecules. The dark blue case is the Earth-like atmosphere, dark red is the Venus-like atmosphere, and the intervening models follow the rainbow sequence with lime green marking the 50:50 case. The abundance of H_2O in the stratosphere does not vary significantly between the two planets due to the condensation to form water clouds on Earth mimicking the dryness of the Venusian atmosphere.

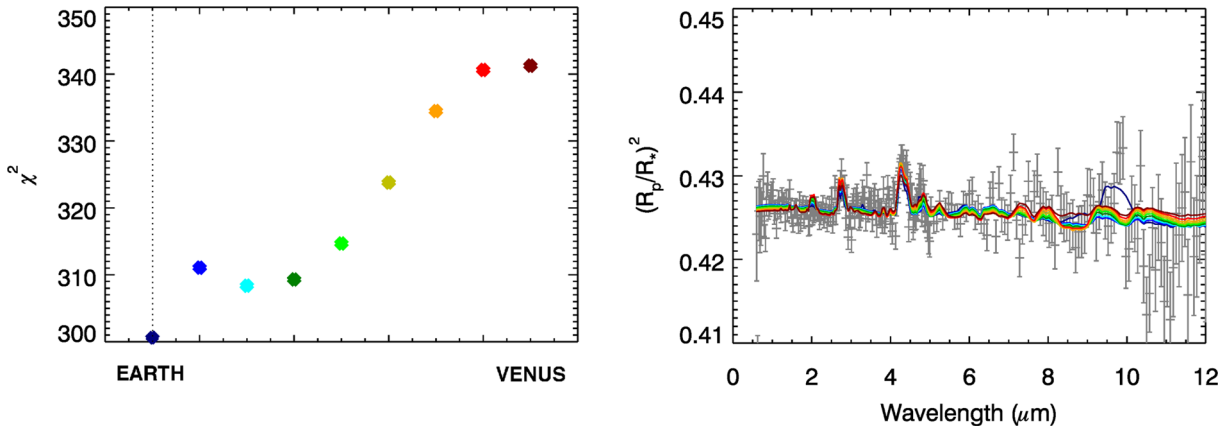


Figure 5. χ^2 goodness of fit measurements and fitted spectra for the Earth case. The lowest χ^2 is marked by a dashed line. The Earth model (dark blue), containing a significant amount of ozone, clearly provides the best fit to the synthetic observation. The location of the ozone feature in the spectrum is indicated by a dashed line.

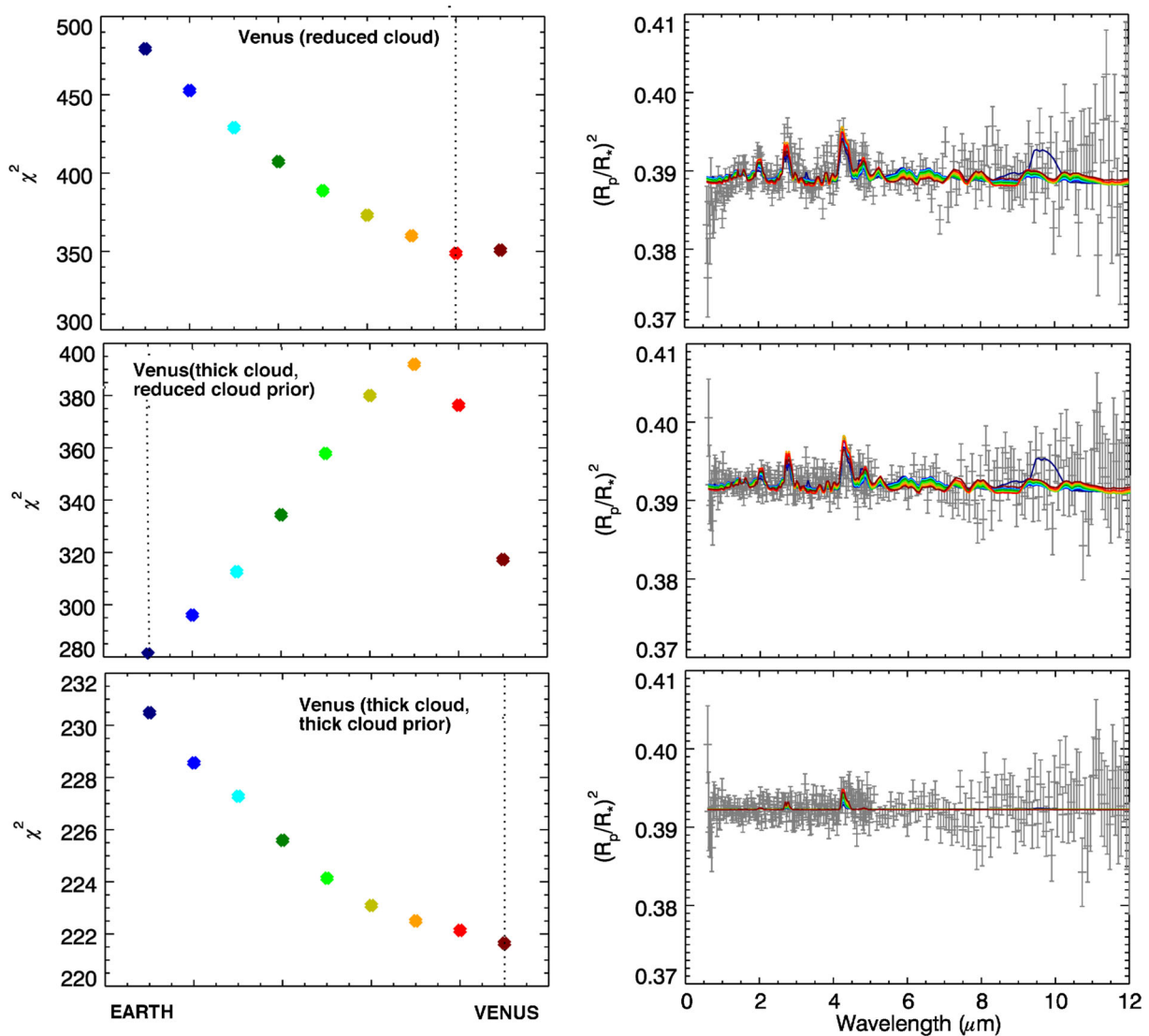


Figure 6. χ^2 goodness of fit measurements and fitted spectra for the reduced-cloud Venus model (top), the cloudy Venus model with a reduced-cloud prior (middle) and the cloudy Venus model with a cloudy prior (bottom). The best-fitting model in each case is indicated by a dashed line on the χ^2 plot. For the cases where the cloud prior used matched the true conditions well, a better fit is found for Venus-type model atmospheres, but in the case where the prior underestimates the cloud optical depth (middle plots) the spectrum would be incorrectly identified as Earth-like.

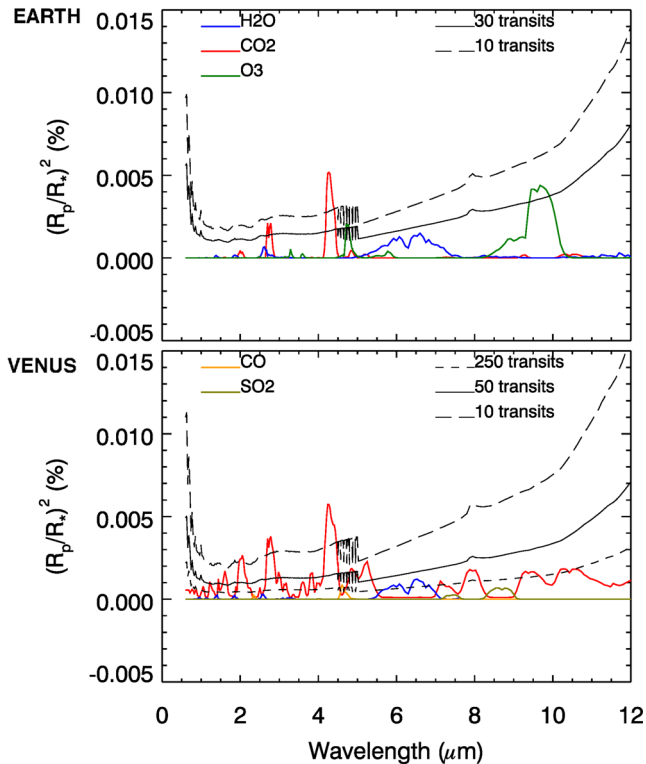


Figure 7. The size of gas absorption features relative to the noise level for the Earth (top) and reduced-cloud Venus (bottom) cases. The sizes of the features are calculated by removing each gas from the full spectrum one at a time and taking the difference between the spectra. For both planets, features are small at short wavelengths as these wavelengths are dominated by clouds and scattering to a greater extent. All features other than CO₂ appear weak for Venus. Around 30 transits is the minimum required to detect O₃ for the Earth case.

feature is also relatively small because the CO₂ abundance is smaller than in any of the other models, hence the Earth model provides the best fit (Fig. 6, middle row).

For the reduced-cloud Venus synthetic observation, Venus-like models provide the best fit to the spectrum, but there is still more ambiguity than there is for the Earth case as the best-fitting model has some Earth-like characteristics. The reason for this is the lack of an ozone-like feature – there is no gas that is present on Venus and not on Earth that also has an unmistakable absorption feature. Whilst SO₂ and OCS fulfil the first part of this criterion, the absorption features are not strong enough to be identified above the noise in the transmission spectra, unlike the Earth O₃ feature. This suggests that, whilst it might be possible to unambiguously spot an ozone-rich planet, detecting an obvious Venus is harder.

We show the size of significant gas features relative to the noise level for the Earth and reduced-cloud Venus cases in Fig. 7, which demonstrates that the Earth case has stronger unique features; the only very strong features for Venus are CO₂ absorption bands, which are also found in Earth’s atmosphere. 250 transits of a Venus-like planet would be required to detect the 6–7 μm H₂O feature, the largest feature after the CO₂ bands, and even then SO₂, a key Venusian gas, is still undetectable. This is partly due to the effect of clouds, but also the fact that the main atmospheric constituent is CO₂, which has a high mean molecular weight and many absorption features that mask the signatures of other gases. The situation is of course even worse for the cloudy-Venus scenario, and clouds are

likely to play a crucial role in the feasibility of constraining Earth-like atmospheres.

7 DISCUSSION

The results presented above rely on the validity of several assumptions made during the modelling process. We consider these assumptions here, and discuss their implications for real observations of M dwarf terrestrial planets.

7.1 Photochemistry and the effect of the M dwarf primary

Throughout this paper, we have assumed that it is possible for two rocky planets close to the liquid water HZ of an M5 star to evolve exactly as Venus and Earth did in the Solar system. However, since it is known that photochemistry has played an important role in the evolution of both atmospheres, and M dwarfs have very different UV fluxes and spectra to G-type stars, this assumption may be flawed. In particular, the formation of the ozone layer on Earth, which is the atmosphere’s most distinctive feature in infrared transmission, is entirely dependent on UV photochemical processes. How likely is it that a similar ozone layer would have formed on an oxygen-rich planet orbiting a cooler star?

Segura et al. (2005) showed that whilst O₃ production would still be expected around a cooler star, the chemical production and destruction processes are very different and the balance is not the same. Grenfell et al. (2013) suggest that the O₃ column abundance around a 3100 K star would be decreased by more than a factor of 3 from the expected abundance around a sun-like star; this is mainly due to the Chapman scheme, the photochemical process responsible for producing the majority of Earth’s ozone, becoming much less efficient. Instead, production due to smog processes dominates, but ozone loss due to the presence of NO_x gases and oxidation of CO is likely to become more efficient, resulting in a net decrease in the O₃ column abundance. Segura et al. (2005) find that the UV flux profile of an active AD Leo-type star would result in the O₃ column abundance being reduced by around 50 per cent, but for a star like GJ 643C it could be increased by the same amount. Rugheimer et al. (2015) find that for models of active M dwarf stars the O₃ column abundance remains relatively high even for later stellar types, due to their high UV fluxes, whereas for an inactive model M5 star the column abundance is decreased by a factor of 20 from the solar value of $\sim 9 \times 10^{18} \text{ cm}^{-2}$ used in our model. Generally, for quiescent stars, the O₃ column depth decreases gradually towards later spectral types. However, the inactive stellar models are presented by Rugheimer et al. (2015) as a limiting case; of the stars with measured UV fluxes discussed in the paper, GJ 876 has a temperature closest to an M5 spectral-type star, and Rugheimer et al. (2015) find that a planet orbiting this star would have an O₃ column abundance of $8.8 \times 10^{17} \text{ cm}^{-2}$, nearly double that of the inactive M5 model.

In Fig. 8, we demonstrate the effect of a reduced ozone column abundance on our ability to distinguish an Earth-like atmosphere from a Venus-like atmosphere. We run the retrieval test with a synthetic observation based on a model with $0.3 \times$ the Earth O₃ abundance, as indicated by Grenfell et al. (2013). It is clear that while the ozone-rich Earth model still provides the best fit to this synthetic observation, it is less straightforward to distinguish the model containing substantial O₃ from other Earth-like models. Assuming the same concentration of oxygen as in Earth’s atmosphere, the lower UV environment around M stars will lead to decreased photochemical production of ozone (e.g. Segura et al. 2005; Rauer et al. 2011; Grenfell et al. 2013; Rugheimer et al. 2015). Therefore

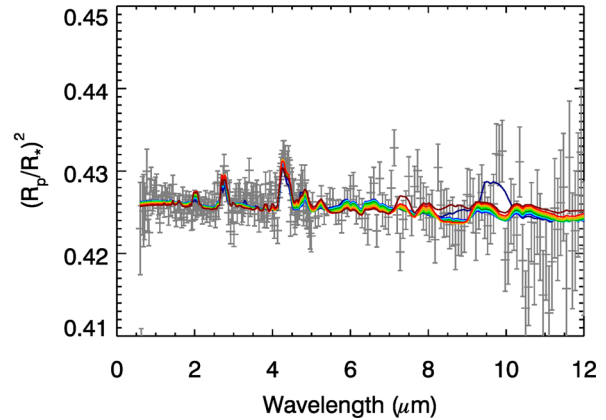
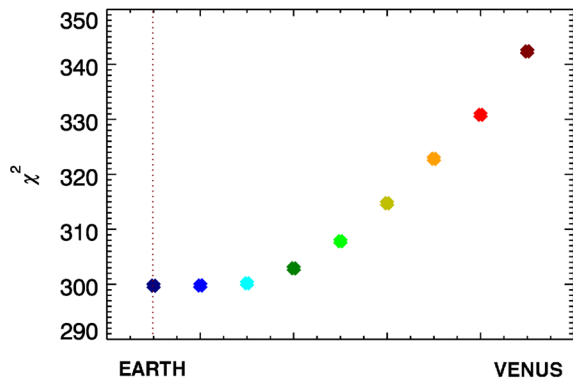


Figure 8. χ^2 goodness of fit measurements and fitted spectra for the Earth case, where the ozone abundance in the synthetic observation is reduced to $0.3 \times$ the true Earth abundance. The Earth model (dark blue) still provides the best fit, but only just. More Earth-like models clearly provide a better fit to the spectrum than Venus-like models, but the ozone absorption signal is no longer large enough to distinguish the true-Earth model from other Earth-like models.

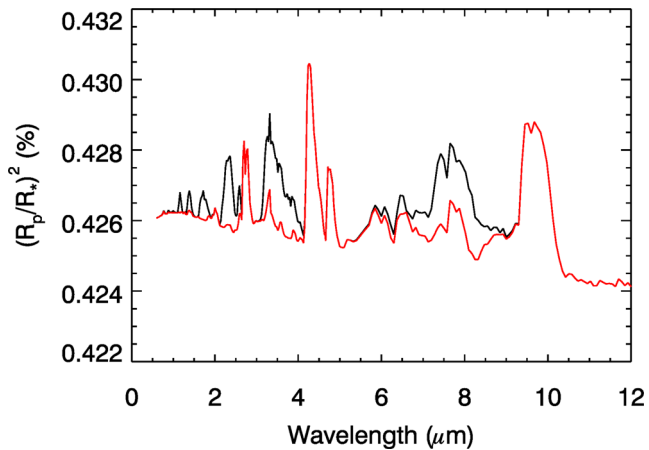


Figure 9. The effect of a factor of 200 increase in CH_4 abundance on the transmission spectrum for an Earth analogue planet. The black line indicates a model with $200 \times \text{CH}_4$, and the red line is the baseline Earth model. The $8 \mu\text{m}$ CH_4 band becomes almost as prominent as the $9 \mu\text{m}$ O_3 feature.

detecting some biosignatures in transit, such as ozone, may be more difficult (Deming et al. 2009; Kaltenegger & Traub 2009), while others, such as methane, may build up to more detectable levels in the atmosphere (Segura et al. 2005; Rugheimer et al. 2015). Some of this effect may perhaps be compensated for by increasing the number of transits observed, but this may introduce other problems (see Section 7.4).

However, photochemistry may not be all bad news for detecting biosignatures around M dwarf planets. In lower UV environments, certain biogenic gases such as CH_4 , N_2O and CH_3Cl have much longer lifetimes and therefore may have higher abundances on those planets for the same biogenic fluxes (Segura et al. 2005; Rauer et al. 2011; Grenfell et al. 2013; Rugheimer et al. 2015), which may mean they would be observable. CH_4 , in particular, could have a mixing ratio of up to $200 \times$ the Earth value, which produces significant changes in the transmission spectrum (Fig. 9). A combination of a reducing biogenic gas and high oxygen abundance indicated by O_3 would be a more convincing indication of the presence of life than a detection of O_3 alone.

Cosmic rays from flaring M dwarf stars can further change the mix of gases present in a planet's atmosphere. Tabataba-Vakili et al. (2016) show that cosmic rays can suppress NO_x gas destruction

of O_3 , and increase HO_x destruction of CH_4 , indicating that long-term observations of M dwarf planet hosts are required. Segura et al. (2010) show that including the effect of protons from M dwarf flares on calculations of O_3 column abundance has significant effects. The detection of flares in a stellar light curve might have a strong bearing on the interpretation of gas abundances measured from transmission spectra. Of course, flaring M dwarf stars may not be the best candidate hosts for Earth-like planets anyway, as the flares may be problematic for the evolution of life on close-in planets. This means that the finding by Rugheimer et al. (2015) that planets orbiting inactive M dwarfs are likely to have weaker O_3 signatures than those orbiting active ones poses some problems for detecting O_3 as a biosignature. However, Segura et al. (2010) suggest that if sufficient O_3 is present in a planet's atmosphere the majority of harmful UV radiation, even from a substantial flare, would be absorbed before reaching the surface, providing an effective shield for any life there. However, the impact of repeated flares on the atmosphere was not tested.

Whilst the case for ozone detection on Earth-like planets might not be so strong when differences in photochemistry are taken into account, the news might be better for a Venus analogue planet. The Venusian clouds are made of sulphuric acid, which is produced photochemically at high altitudes. Different UV photon fluxes, in much the same way as they alter ozone production, may also inhibit (or enhance) sulphuric acid photolysis. This may either increase the likelihood of a Venus analogue being relatively cloud-free, which makes detection of gas absorption features easier, or increase the production of sulphur aerosol, which may lead to an even flatter spectrum.

Finally, a persistent issue in transiting exoplanet studies is that the star must be very well characterized if the derived planet parameters are to be reliable, since all measurements are relative to the size and mass of the star. For many M stars, these properties are still not known to high precision. It will therefore be necessary to study an M dwarf primary in detail before attempting to characterize its companion.

7.2 Abiotic false positives

On the Earth, the observable abundance of O_3 arises directly from the large fraction of atmospheric O_2 , which in turn arises from biological processes. However, observing a similar abundance of O_3

on an exoplanet would not necessarily imply biological activity, as there are several potential abiotic processes that could also generate substantial amounts of O_2 . Domagal-Goldman et al. (2014) model abiotic O_2 , O_3 and CH_4 production from photolysis for planets orbiting a range of stars, and find that planets irradiated by an F2V star such as σ Bootis would have O_3 column abundances only $\sim 7 \times$ smaller than present Earth's. Signatures of this size might be detectable in transit with *JWST*. However, M dwarf host scenarios tested did not produce such large amounts of O_2 and O_3 , with O_3 column abundances a factor of 1000 lower. Tian et al. (2014) find that M dwarf hosts with high (~ 1000 super solar) FUV/UV flux ratios could also produce substantial amounts of O_2 and O_3 (O_3 abundances up to $0.05 \times$ present-day Earth) without the requirement for biological processes. Since, as stated above, O_3 from Earth levels of biogenic oxygen could be substantially reduced around M dwarf hosts, distinguishing between the upper limit of abiotic O_3 and the lower bound of biologically related O_3 could potentially be very difficult.

Luger & Barnes (2015) postulate another abiotic production mechanism for substantial amounts of O_2 . Earth-sized planets with a water ocean may lose those oceans through evaporation if they undergo a runaway greenhouse. Photodissociation of water vapour can then occur, and hydrogen is preferentially lost to space over the heavier oxygen. This can lead to a build-up of O_2 in the atmosphere, even up to several hundred bars. Whilst the authors do not discuss O_3 chemistry under these circumstances, it is conceivable that significant amounts could be produced. Wordsworth & Pierrehumbert (2014) point out that H_2O -rich atmospheres without significant amounts of non-condensing gas, such as N_2 , are particularly vulnerable to this process, as the non-condensing gas creates a cold trap for H_2 that aids retention. Other abiotic O_2 production mechanisms are also possible (e.g. Narita et al. 2015).

7.3 Refraction and multiple scattering

Currently, the *NEMESIS* model does not account for refraction of transmitted light in the lower atmosphere of a transiting planet. This is relatively unimportant for hot Jupiters, which are high temperature and hydrogen-rich, but the effect is enhanced for cooler planets. However, the size of the effect is also correlated with the size of the star, so it is less important for cool planets around small M dwarfs than similar planets around sun-like stars. Bétrémieux & Kaltenegger (2014) find that there is very little difference between synthetic Earth spectra with and without refraction if the planet is assumed to be in orbit around a star between M5 and M9 spectral types. The differences are certainly far below the level of the noise on the synthetic spectra discussed in this work. By contrast, there are substantial differences for a true Earth-analogue orbiting a sun-like star, further reinforcing the point that studying transiting Earth and Venus analogues around cooler stars is much more straightforward.

For primary transit, *NEMESIS* uses an extinction-only approximation for any scattering particles in the atmosphere. This is justified because of the extremely long path length in primary transit, which makes it likely that most photons encountering optically thick cloud will either be absorbed or scattered out of the beam. However, this does not take into account cloud particles with strongly forward-scattering phase functions. The sulphuric acid cloud on Venus is known to be strongly forward scattering, so it is possible that in the cloudy Venus calculation we are underestimating the amount of starlight that penetrates the atmosphere at pressures below the cloud top. de Kok & Stam (2012) demonstrate this effect for Titan by comparing Monte Carlo photon-firing models that

(1) do not include multiple scattering, and (2) account for multiple scattering in strongly forward-scattering clouds. They find that the CH_4 and aerosol abundance is consistently underestimated for the non-multiple-scattering case, by a factor of around 0.92. However, we judge that the effects seen on the spectrum are likely to be small compared with the noise on the transmission spectra considered here.

7.4 Temporal changes

So far, the transit spectroscopy technique has relied on it being possible to observe several transits of a planet and combine the data from each observation to increase the signal-to-noise ratio. This is a legitimate approach only if the stellar and atmospheric conditions are not expected to vary greatly between observations. In the case of an M dwarf, it is likely that starspots will be present, although with the relatively slow rotation period spot coverage should not change appreciably during a transit. However, given that several tens of observations are required for each planet, stellar activity may limit reliable combination of multiple transits. It may be possible to compensate for these effects if the star is monitored by an independent programme, as was done for the K star HD 189733 during the observational campaigns that resulted in the overview presented in Pont et al. (2013). The effect of star spots decreases at longer wavelengths, so detection of the ozone feature would probably not be affected, but it would be much more difficult to place constraints on a Venus-like atmosphere where most observable features are at wavelengths shorter than $5 \mu m$.

When terrestrial planets are under consideration, it is also necessary to account for possible temporal variations in the planet's atmosphere, especially in cloud properties. Whilst the Venusian cloud layer is very stable, a Venus analogue with reduced cloud opacity might not have such constant cloud cover. If the amount of cloud cover changes between observations, it might become impossible to combine spectra in any useful way as the size of absorption features would vary between observations – this can be seen in Fig. 6 comparing the top and bottom spectral plots.

The cloud cover on Earth also changes from day to day, although as the Earth cloud forms deeper in the atmosphere it has a smaller effect on the spectrum. However, certain events on Earth can cause dramatic changes in cloud and haze. For example, large volcanic eruptions such as Mount Pinatubo in 1992 are capable of increasing aerosol optical depth in the atmosphere on a global scale (Self et al. 1996), and this could have a significant effect on transmission spectra. Earth and Venus analogues around M5 stars would be in sufficiently close orbits to be within the tidal locking radius. Strong tidal forces may increase the rate of volcanic activity on these planets, possibly increasing the frequency of Pinatubo-size eruptions.

In addition, the molecular features of interest could also vary in strength between observations. Segura et al. (2010) find that the O_3 column depth can vary by large amounts during a strong flare from an active M dwarf, especially when the effect of protons is accounted for. Attempting to average over repeated observations for a flaring M dwarf would therefore be problematic.

8 CONCLUSIONS

Whilst it is possible to identify strong absorption features, due to gases such as O_3 , in *JWST* transit measurements of M dwarf Earth analogues, there are many complicating factors. A reduced O_3 abundance compared with the Earth case, which seems to be likely

considering the different UV flux for M stars compared with G stars, would make it harder to unambiguously identify the presence of ozone. The presence of high cloud on Venus analogue planets means that gas absorption features could be almost completely obscured, making it very difficult to identify the atmospheric constituents and obfuscating attempts to characterize the planet. Less cloudy Venus-like planets, which may be more likely to occur around cooler stars, would be much more favourable for characterization.

More generally, characterizing planets orbiting variable stars is difficult if multiple observations are needed to boost the signal. This is further complicated in the case of terrestrial planets, as their global atmospheric characteristics may also change on short time-scales. Given the level of time investment required in observing this kind of target with *JWST*, a very careful cost-benefit analysis would need to be completed for any such observation to be approved. Given the likelihood of signal disruption due to stellar activity or planet temporal variability, and the strong possibility that the planet will be cloudy, we recommend that the following criteria are fulfilled before such an observation is considered.

(i) The Earth-like planet candidate is in a low-eccentricity orbit around a nearby (< 10 pc) red dwarf with a spectral type of around M5.

(ii) The host star is relatively quiet for its spectral type, with the caveat that stars with very low UV fluxes would be less likely to host planets with observable O_3 .

(iii) The host star can be periodically monitored for activity variations throughout the duration of *JWST* observations.

(iv) The target is the most favourable of its type, as it is likely that only one to two terrestrial planets can command this level of investment.

(v) The mass and radius of both the planet and star have been measured to high precision (so the density of the planet is known).

Although obtaining transit spectra of terrestrial planets is difficult, the first characterization of a cool, compact, terrestrial atmosphere would result in significant scientific return. If the criteria mentioned above can be met for an Earth-like planet candidate, we would advocate investing the required *JWST* observing time.

ACKNOWLEDGEMENTS

JKB and PGJ acknowledge the support of the Science and Technology Facilities Council. LNF is supported by a Royal Society University Research Fellowship. We thank Victoria Meadows for pointers towards useful literature, and the anonymous reviewer whose constructive comments substantially improved the paper.

REFERENCES

Abe Y., Abe-Ouchi A., Sleep N. H., Zahnle K. J., 2011, *Astrobiology*, 11, 443
 Barstow J. K. et al., 2012, *Icarus*, 217, 542
 Barstow J. K., Aigrain S., Irwin P. G. J., Bowles N., Fletcher L. N., Lee J.-M., 2013a, *MNRAS*, 430, 1188
 Barstow J. K., Aigrain S., Irwin P. G. J., Fletcher L. N., Lee J.-M., 2013b, *MNRAS*, 434, 2616
 Barstow J. K., Aigrain S., Irwin P. G. J., Kendrew S., Fletcher L. N., 2015, *MNRAS*, 448, 2546
 Benneke B., Seager S., 2012, *ApJ*, 753, 100
 B  tr  mieux Y., Kaltenecker L., 2014, *ApJ*, 791, 7
 de Kok R. J., Stam D. M., 2012, *Icarus*, 221, 517

Deming D. et al., 2009, *PASP*, 121, 952
 Domagal-Goldman S. D., Segura A., Claire M. W., Robinson T. D., Meadows V. S., 2014, *ApJ*, 792, 90
 Donahue T. M., Hoffman J. H., Hodges R. R., Watson A. J., 1982, *Science*, 216, 630
 Ehrenreich D. et al., 2012, *A&A*, 537, 2
 Esposito L. W., Knollenberg R. G., Marov M. I., Toon O. B., Turco R. P., 1983, in Hunten D. M., Colin L., Donahue T. M., Moroz V., eds, *The Clouds are Hazes of Venus*. Univ. Arizona Press, Tucson, p. 484
 Goody R. M., Yung Y. L., 1989, *Atmospheric Radiation : Theoretical Basis*. Oxford Univ. Press, NY
 Grenfell J. L. et al., 2013, *Astrobiology*, 13, 415
 Griffith C. A., 2014, *Phil. Trans. R. Soc. A*, 372, 20130086
 Hamann U. et al., 2014, *Atmos. Meas. Tech.*, 7, 2839
 Hansen J. E., Hovenier J. W., 1974, *J. Atmos. Sci.*, 31, 1137
 Irwin P. G. J. et al., 2008, *J. Quant. Spectrosc. Radiat. Transfer*, 109, 1136
 Irwin P. G. J., Barstow J. K., Bowles N. E., Fletcher L. N., Aigrain S., Lee J.-M., 2014, *Icarus*, 242, 172
 Kaltenecker L., Traub W. A., 2009, *ApJ*, 698, 519
 Kendrew S. et al., 2015, *PASP*, 127, 623
 Kopparapu R. K. et al., 2013, *ApJ*, 765, 131
 Kreidberg L. et al., 2014, *Nature*, 505, 69
 L  cis A. A., Oinas V., 1991, *J. Geophys. Res.*, 96, 9027
 Leconte J., Forget F., Charnay B., Wordsworth R., Selsis F., Millour E., Spiga A., 2013, *A&A*, 554, A69
 Luger R., Barnes R., 2015, *Astrobiology*, 15, 119
 Madhusudhan N., Crouzet N., McCullough P. R., Deming D., Hedges C., 2014, *ApJ*, 791, L9
 Myhre C. E. L., Christensen D. H., Nicolaisen D. H., Neilsen C. J., 2003, *J. Phys. Chem.*, 107, 1979
 Narita N., Enomoto T., Masaoka S., Kusakabe N., 2015, *Nature Sci. Rep.*, 5, 13977
 Palmer K. F., Williams D., 1975, *Appl. Opt.*, 14, 208
 Pollack J. B. et al., 1974, *Icarus*, 23, 8
 Pont F., Sing D. K., Gibson N. P., Aigrain S., Henry G., Husnoo N., 2013, *MNRAS*, 432, 2917
 Rasool S. I., de Bergh C., 1970, *Nature*, 226, 1037
 Rauer H. et al., 2011, *A&A*, 529, A8
 Redfield S., Endl M., Cochran W. D., Koesterke L., 2008, *ApJ*, 673, L87
 Ricker G. R. et al., 2015, *J. Astron. Telesc. Instrum. Syst.*, 1, 014003
 Rodgers C. D., 2000, *Inverse Methods for Atmospheric Sounding*. World Scientific, Singapore
 Rothman L. S. et al., 2009, *J. Quant. Spectrosc. Radiat. Transfer*, 110, 533
 Rugheimer S., Kaltenecker L., Segura A., Linsky J., Mohanty S., 2015, *ApJ*, 809, 57
 Segura A., Kasting J. F., Meadows V., Cohen M., Scalo J., Crisp D., Butler R. A. H., Tinetti G., 2005, *Astrobiology*, 5, 706
 Segura A., Walkowicz L. M., Meadows V., Kasting J., Hawley S., 2010, *Astrobiology*, 10, 751
 Seiff A., Schofield J. T., Kliore A. J., Taylor F. W., Limaye S. S., 1985, *Adv. Space Res.*, 5, 3
 Self S., Zhao J.-X., Holasek R. E., Torres R. C., King A. J., 1996, in Newhall C., Punongbayan R., eds, *FIRE and MUD: Eruptions and Lahars of Mount Pinatubo*, Philippines. Univ. Washington Press, Seattle
 Tabataba-Vakili F., Grenfell J. L., Grieblmeier J.-M., Rauer H., 2016, *A&A*, 585, A96
 Taylor F., Grinspoon D., 2009, *J. Geophys. Res.*, 114, E00B40
 Tian F., France K., Linsky J. L., Mauas P. J. D., Vieytes M. C., 2014, *Earth Planet. Sci. Lett.*, 385, 22
 Wakeford H. R. et al., 2013, *MNRAS*, 435, 3481
 Wheatley P. J. et al 2013, in Saglia R., ed., *EPJ Web Conf.*, 47, *The Next Generation Transit Survey (NGTS). Hot Planets and Cool Stars*, p. 13002
 Wordsworth R., Pierrehumbert R., 2014, *ApJ*, 785, L20
 Zsom A., Seager S., de Wit J., Stamenkovi   V., 2013, *ApJ*, 778, 109

This paper has been typeset from a $\text{\TeX}/\text{\LaTeX}$ file prepared by the author.